THE JOURNAL OF PHYSICAL CHEMISTRY B

Article

pubs.acs.org/JPCB

Molecular Density Functional Theory: Application to Solvation and Electron-Transfer Thermodynamics in Polar Solvents

Daniel Borgis,*[,†] Lionel Gendre,[‡] and Rosa Ramirez[‡]

[†]Laboratoire PASTEUR, UMR 8640 CNRS-ENS-UPMC, Ecole Normale Supérieure, 24 rue Lhomond, 75231 Paris, France

[‡]Laboratoire LAMBE, CNRS-UMR 8587, Université Evry-Val-d'Essonne, Bd François Mitterand, 91025 Evry, France

ABSTRACT: A molecular density functional theory of solvation is presented. The solvation properties of an arbitrary solute in a given solvent, both described by a molecular force field, can be obtained by minimization of a position- and orientation-dependent free-energy density functional. In the homogeneous reference fluid approximation, the unknown excess term of the functional can be approximated by the angular-dependent direct correlation function of the pure solvent. This function can be extracted from a preliminary MD simulation of the pure solvent by computing the angular-dependent pair distribution function and solving subsequently the molecular Ornstein–Zernike equation. The corresponding functional can then be minimized on a three-dimensional cubic grid for positions and a Gauss–Legendre angular grid for orientations to provide the solvation free energy of embedded molecules at the same time as the solvent three-dimensional microscopic structure. This functional minimization procedure is much more efficient than direct molecular dynamics simulations combined with thermodynamic integration schemes. The approach is shown to be also pertinent to the molecular-level determination of electron-transfer properties such as reaction free energy and reorganization energy. It is illustrated for molecular solvation and photochemical electron-transfer reactions in acetonitrile, a prototypical polar aprotic solvent.

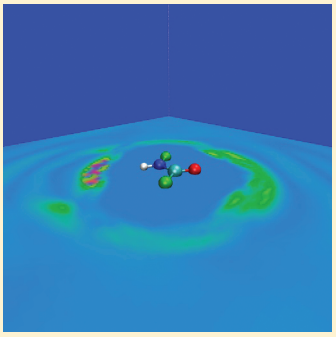

1. INTRODUCTION

The molecular-level prediction of the solvation free energy of molecular solutes in molecular solvents and the determination of the thermodynamics quantities governing charge-transfer rates in solution, the so-called reaction free energy and reorganization energy, are problems of primary importance in physical chemistry and biology.

Two extreme strategies can be found in the literature to compute free energies. The so-called explicit-solvent method consists of using molecular simulation techniques such as molecular dynamics (MD) or Monte Carlo (MC) with an atomistic solvent model. There are a number of well-established statistical mechanics techniques to estimate absolute or relative free energies by molecular simulations,[1] for example, thermodynamic integration methods based on umbrella sampling[2,3] or generalized constraints.[4,5] See, for example, ref 6 for their application to the systematic computation of molecules' solvation free energies. In any case, this type of calculations remains extremely costly; it requires one to consider a sufficiently large number of solvent molecules around the molecular solute and, for this large system, to compute a "generalized force" over many microscopic solvent configurations for many different points along the integration path.

Another class of methods, known as implicit solvent models,[7,8] relies on the assumption that the macroscopic laws remain valid at a microscopic level and that solvation free energies can be computed by combining a dielectric continuum description of the solvent outside of the solute core and a simple solvent-accessible surface area expression for the nonelectrostatic contributions.[9] For the electrostatic part, the stationary Poisson–Boltzmann equation can be solved for the electrostatic potential using sharp definitions of the dielectric boundaries and various efficient numerical techniques,[8] making it possible to handle very large biomolecular systems.[10] Density functional methods based on the minimization of the polarization density[11] or polarization charge density[12,13] have been introduced too. There are serious limitations however to a continuum dielectric approach and, first of all, the validity of the macroscopic electrostatic laws at microscopic distances, the neglect of the molecular nature of the solvent, and the ambiguous definition of all of the nonelectrostatic energetic contributions, such as hydrophobicity. Macroscopic approaches to hydrophobicity, which mix consistently with the Poisson–Boltzmann description, are presently developed.[14,15] More advanced implicit methods relying on the statistical mechanics of molecular liquids have been developed too, and these are able to cope with the molecular nature of the solvent without considering explicitly all of its instantaneous microscopic degrees of freedom. Among possible approaches, let us mention molecular integral equation theories in the reference interaction site (RISM),[16−23] the molecular[24−30] or the mixed[31,32] picture, Gaussian field theories,[33−36] the density functional theory (DFT) of molecular liquids,[37−49] or, finally, field theoretical approaches to dipolar solvent–ion mixtures, which lead to a

Received: November 10, 2011
Revised: January 16, 2012
Published: January 23, 2012

generalization of the Poisson−Boltzmann equation accounting for particle size and dielectric saturation.[50−54]

Concerning charge-transfer reactions in solution, most of our vision of charge-transfer processes in solution comes from the Marcus electron-transfer theory based on a dielectric continuum description of the solvent.[55−57] This approach has been extended in many aspects and applied to the study of a number of electron- and proton-transfer reactions in various media.[58−60] In the original Marcus view,[55] the solvent is described by a nonequilibrium polarization field obeying a quadratic free-energy functional (the so-called Marcus functional[11]). The subsequent generalization of the Marcus theory beyond continuum electrostatics has gone in two complementary direction. Again, an explicit solvent computational route, pioneered by Warshel[61] and applied to many chemical or biochemical electron- and proton-transfer processes ever-since,[62−70] consists of adopting a fully atomistic description of the charge transfer plus solvent system and using molecular simulations to characterize the charge-transfer energetics, including the reaction free energy and solvent reorganization free energy. Most of those calculations make use of the Gaussian property of the electrostatic energy gap fluctuations, which is at the heart of Marcus theory and could be verified many times at a microscopic level.[62−65,68,70] This assumption makes it possible to simplify the calculations and to bypass the costly direct calculation of the reaction free energy. On the other hand, analytical extension of Marcus theory has been proposed that generalizes the Marcus electrostatic functional to account for finer microscopic effects, in particular, the nonlocal (or k-dependent) character of the static dielectric constant. There have been a number of theoretical works devoted to the study of the static dielectric constant $\epsilon(k)$ of polar fluids, of the corresponding frequency-dependent quantity $\epsilon(k,\omega)$ (including longitudinal and transverse components), and of the implication of those microscopic quantities for the energetics and dynamics of charge-transfer processes.[71−84]

We have introduced previously a three-dimensional molecular density functional theory (MDFT) approach to solvation in generic[44−46] as well as realistic[47,48] polar solvents. We showed that the classical density functional theory of molecular liquids, formulated in the molecular picture where each solvent molecule is characterized as a rigid entity by the position of its center of mass and its orientation, provides a universal and flexible tool to devise realistic "implicit solvent" models based on a full molecular solvent representation. We introduced the name of MDFT[48] in reference to the molecular Ornstein−Zernike (MOZ) integral equation theory[26−30] and in contrast to RISM approaches based all along on an interaction-site picture. This approach can be implemented in a practical way by using a discrete representation of the solvent density in both positions and orientations to predict the solvation free energy of arbitrary molecular solutes in arbitrary solvents, at the same time providing the microscopic three-dimensional solvent structure around the solute.[47,48] In ref 46, we advocated the use of MDFT for charge-transfer reactions in polar solvents. This question constitutes the main focus of the present work.

The ability of MDFT to cope with solvation and charge-transfer properties at the molecular level is illustrated in this paper for the case of acetonitrile, a solvent that has been a paradigm for many experimental and computational studies of charge-transfer processes in polar aprotic solvents. The relevance of the approach will be assessed systematically by comparison to reference MD simulations.

The paper is organized as follows. Section 2 describes briefly the principles of MDFT and its developments in the context of molecular solvation and electron-transfer reactions. Section 3 presents the application to a molecular model of acetonitrile, discusses how to compute the direct correlation functions of the pure solvent, and discusses how to minimize numerically the associated functional to get the microscopic solvation properties of a series of ground- or excited-state molecular solutes. Section 4 concludes.

2. DENSITY FUNCTIONAL THEORY OF SOLVATION

2.1. Solvation Free Energy. We begin by recalling the basis of the density functional theory of liquids and discussing the general problem of a molecular solvent submitted to an external field, which, in our case, is created by a molecular solute of arbitrary shape dissolved at infinite dilution in the solvent. The individual solvent molecules are considered to be rigid bodies described by their position $\mathbf{r}$ and orientation Ω (in terms of three Euler angles θ, ϕ, ψ). The solute and solvent are described in all microscopic details by a molecular "force field" involving atomic Lennard-Jones and partial charge parameters. Given that the solute is fixed and defined by the position, $\mathbf{r}_i$, of its different atomic sites, the external potential $V_{ext}(\mathbf{r},\Omega)$ exerted on a solvent molecule with coordinates $(\mathbf{r},\Omega)$ is thus defined as

$$V_{ext}(\mathbf{r},\Omega) = \sum_{i\in\text{solute}} \sum_{j\in\text{solvent}} 4\epsilon_{ij}\left[\left(\frac{\sigma_{ij}}{r_{ij}}\right)^{12} - \left(\frac{\sigma_{ij}}{r_{ij}}\right)^{6}\right] + \frac{q_i q_j}{4\pi\epsilon_0 r_{ij}} \quad (1)$$

where ϵ_{ij} and σ_{ij} are the Lennard-Jones parameters between solute site i and solvent site j and q_i and q_j are the partial charges carried by those sites. The relative site−site vectors are a function of the solvent molecule position and orientation and defined as $\mathbf{r}_{ij} = \mathbf{r} + \mathbf{R}(\Omega)\mathbf{s}_j - \mathbf{r}_i$, where $\mathbf{s}_j$ denotes the site positions in the molecular frame and $\mathbf{R}(\Omega)$ is the rotation matrix associated with Ω.

The grand potential density functional for a fluid having an inhomogeneous density $\rho(\mathbf{r},\Omega)$ in the presence of an external field $V_{ext}(\mathbf{r},\Omega)$ can be evaluated relative to a reference homogeneous fluid having the same chemical potential μ_s and the density $\rho_0 = n_0/8\pi^2$ (or $n_0/4\pi$ for linear molecules), n_0 being the particle number density

$$\Theta[\rho] = \Theta[\rho_0] + \mathcal{F}[\rho] \quad (2)$$

Following the general theoretical scheme introduced by Evans,[37,39,85] the density functional $\mathcal{F}[\rho]$ can be split into three contributions, an ideal term (id), an external potential term describing the interaction between the solvent and the dissolved molecule (ext), and an excess free-energy term accounting for the intrinsic interactions within the fluid (exc)

$$\mathcal{F}[\rho] = \mathcal{F}_{id}[\rho] + \mathcal{F}_{ext}[\rho] + \mathcal{F}_{exc}[\rho] \quad (3)$$

dx.doi.org/10.1021/jp210817s | J. Phys. Chem. B 2012, 116, 2504−2512

with the following expressions for each term

$$\mathcal{F}_{id}[\rho] = k_B T \int d\mathbf{r}\, d\Omega \left[\rho(\mathbf{r}, \Omega) \ln\left(\frac{8\pi^2 \rho(\mathbf{r}, \Omega)}{n_0} \right) - \rho(\mathbf{r}, \Omega) + \frac{n_0}{8\pi^2} \right] \quad (4)$$

$$\mathcal{F}_{ext}[\rho] = \int d\mathbf{r}\, d\Omega\, V_{ext}(\mathbf{r}, \Omega)\rho(\mathbf{r}, \Omega) \quad (5)$$

$$\mathcal{F}_{exc}[\rho] = -\frac{1}{2} k_B T \int\int d\mathbf{r}\, d\mathbf{r}'\, d\Omega\, d\Omega'\, \Delta\rho(\mathbf{r}, \Omega) c(|\mathbf{r} - \mathbf{r}'|, \Omega, \Omega')\Delta\rho(\mathbf{r}', \Omega') + \mathcal{F}_{cor}[\rho] \quad (6)$$

where $\Delta\rho(\mathbf{r},\Omega) = \rho(\mathbf{r},\Omega) - \rho_0$. In the last equation, the first term represents the homogeneous reference fluid (HRF) approximation, where the excess free-energy density is written in terms of the angular-dependent direct correlation of the pure solvent. The second term represents the unknown correction, which can be expressed as a systematic expansion in terms of the three-body, ..., n-body terms' direct correlation functions of the pure solvent.[37] In this work, we suppose that $\mathcal{F}_{cor}[\rho] = 0$, that is, we limit ourselves to the HRF approximation, which is known to be equivalent to the HNC approximation in integral equation theories.[37] This approximation was shown to fall short for associated liquids such as water.[30,48,49]

In the HRF approximation, the above functional can be minimized according to

$$\frac{\delta\mathcal{F}}{\delta\rho} = \beta^{-1} \ln\left(\frac{\rho(\mathbf{r}, \Omega)}{\rho_0} \right) + V_{ext}(\mathbf{r}, \Omega) + V_{exc}(\mathbf{r}, \Omega) = 0 \quad (7)$$

with the definition of the excess potential

$$V_{exc}(\mathbf{r}_1, \Omega_1) = -k_B T \int d\mathbf{r}_2\, d\Omega_2\, c(\mathbf{r}_{12}, \Omega_1, \Omega_2) \Delta\rho(\mathbf{r}_2, \Omega_2) = -k_B T\, FT^{-1}[\int d\Omega_2\, c(\mathbf{k}, \Omega_1, \Omega_2) \Delta\rho(\mathbf{k}, \Omega_2)] \quad (8)$$

that appears as a convolution and can be computed using Fourier transforms. At this point, we are faced with the problem of knowing the direct correlation function $c(\mathbf{r}_{12},\Omega_1,\Omega_2)$ of the homogeneous reference fluid. Having in hand an atomistic model for the solvent, this can be done in principle by computing first the pair correlation function $h(\mathbf{r}_{12},\Omega_1,\Omega_2)$ of the homogeneous solvent using "exact simulation methods" such as Monte Carlo or molecular dynamics simulations and then inverting the MOZ integral equation, which relates the functions h and c in the laboratory frame

$$h(\mathbf{r}_{12}, \Omega_1, \Omega_2) = c(\mathbf{r}_{12}, \Omega_1, \Omega_2) + \rho_0 \int d\mathbf{r}_3\, d\Omega_3\, h(\mathbf{r}_{13}, \Omega_1, \Omega_3)c(\mathbf{r}_{32}, \Omega_3, \Omega_2) \quad (9)$$

or in Fourier space

$$h(\mathbf{k}, \Omega_1, \Omega_2) = c(\mathbf{k}, \Omega_1, \Omega_2) + \rho_0 \int d\Omega_3\, h(\mathbf{k}, \Omega_1, \Omega_3)c(\mathbf{k}, \Omega_3, \Omega_2) \quad (10)$$

In order to manage the inversion problem, it has been shown that both the pair distribution function and the direct correlation function can be expanded into a basis of rotational invariants.[24] Blum[24,25] and later Patey[26] have shown how to solve the angular dependent OZ equations in **k**-space using Hankel transforms. This is the basis of the MOZ integral equation theory of anisotropic fluids.[29,30] We showed in ref 47 that this equation can also be solved using angular grids to handle the orientational dependence and to provide the function $c(\mathbf{k},\Omega_1,\Omega_2)$ as an input to the density functional. Due to the finite box size used in molecular simulations, this inversion procedure is ill-defined at very small k values (typically below 1 Å^{-1}); we show in the Appendix how exact relations linking the c-function to the fluid macroscopic properties can be exploited to complement this function close to $\mathbf{k} = 0$.

With the solvent direct correlation function, $c(\mathbf{k},\Omega_1,\Omega_2)$, being known in **k**-space, the functional can be minimized numerically using a discretized representation of $\rho(\mathbf{r},\Omega)$, with **r** represented on a cubic three-dimensional lattice and Ω on a Gauss–Legendre grid. This procedure provides, at the minimum, the solvation free energy of the solute, F_{eq}, as well as the microscopic solvent structure, in terms of the complete position and angular density, $\rho_{eq}(\mathbf{r},\Omega)$.

2.2. Electron Transfer Free Energy and Reorganization Energy. We now consider a dissolved molecular system undergoing a charge-transfer reaction (be it spontaneous or light-induced), going from a reactant electronic charge distribution 1 to a product one, labeled 2. This process can be depicted by the two-state Marcus picture of Figure 1,

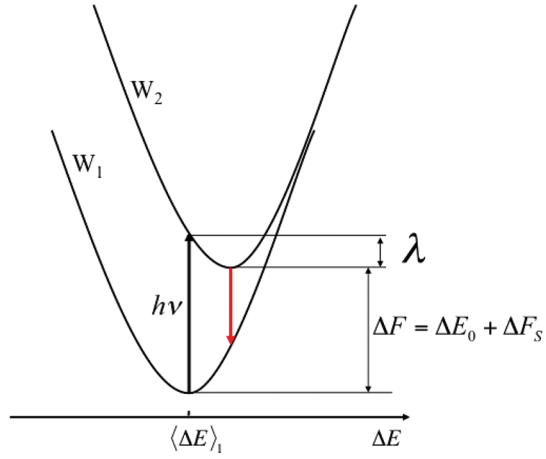

Figure 1. Marcus representation of the diabatic free-energy curves, $W_{1,2}$, as function of the microscopic solvent energy gap ΔE for an electron-transfer reaction, here for a photochemical reaction in the so-called inverted regime. The black upward arrow indicates the Franck–Condon vertical excitation energy, whereas the downward one indicates the nonadiabatic relaxation at the excited-state surface minimum. All other notations are defined in the text.

showing the free-energy curves of states 1 or 2 as a function of the solvent coordinate; the standard choice is the energy gap coordinate, the difference in solute/solvent interaction energies between states 1 and 2 for a given microscopic solvent configuration. The figure shows the two quantities of importance to describe the equilibrium and rate constants of the reaction, the reaction free energy ΔF, and the

dx.doi.org/10.1021/jp210817s | J. Phys. Chem. B 2012, 116, 2504–2512

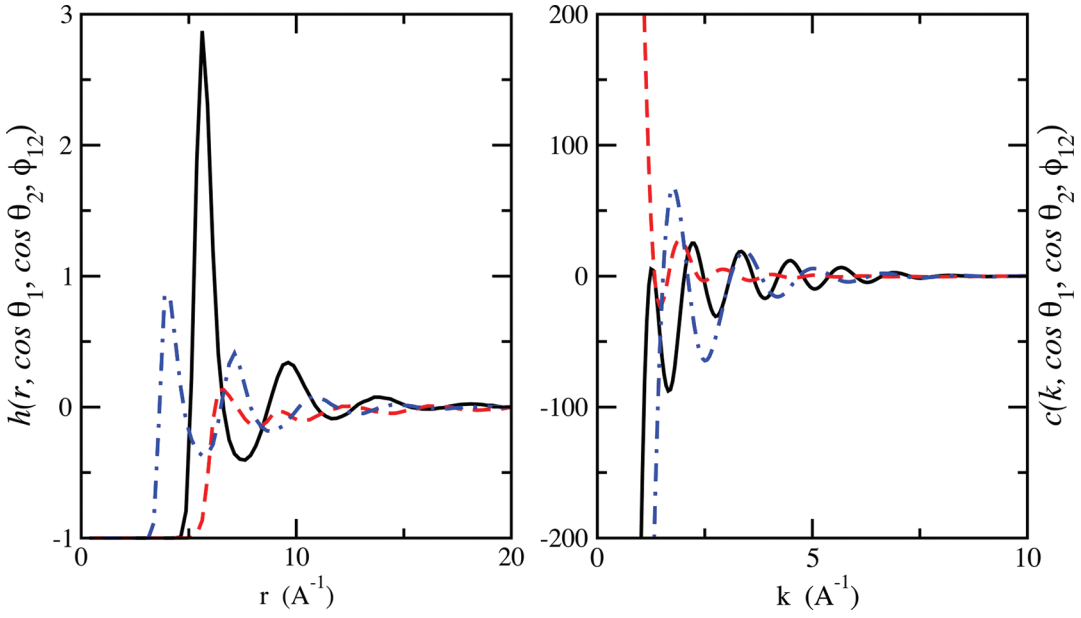

Figure 2. (Left) Pair distribution function of acetonitrile computed in the intermolecular frame for different orientations, cos $\theta_1 = 1$, cos $\theta_2 = 1$, $\phi_{12} = 0$ (solid line), cos $\theta_1 = -1$, cos $\theta_2 = 1$, $\phi_{12} = 0$ (dashed line), and cos $\theta_1 = 0$, cos $\theta_2 = 0$, $\phi_{12} = 0$ (dotted−dashed line). (Right) Direct correlation function in the **k**-frame for the same orientations and with the same symbols.

reorganization energy, λ. There is a ample literature on how to compute those quantities using molecular simulations.

From a MDFT perspective, the two molecular states generate two different external potentials, $V_1(\mathbf{r},\Omega)$ and $V_2(\mathbf{r},\Omega)$. Minimization of the functional with each of them will provide the absolute solvation free energy of each molecular state and by consequence

$$\Delta\mathcal{F} = \Delta E_0 + \Delta F_S = \Delta E_0 + F_{eq}^2 - F_{eq}^1 \tag{11}$$

where ΔE_0 is the intrinsic free-energy difference of the reaction and ΔF_S is the solvation free-energy contribution.

Furthermore, it can be readily shown that each separate minimization can provide in addition the averaged energy gap in each state, that is

$$\langle \Delta E\rangle_n = \Delta E_0 + \langle \Delta V\rangle_n = \Delta E_0 + \int d\mathbf{r}\, d\Omega\, (V_2(\mathbf{r},\Omega) - V_1(\mathbf{r},\Omega))\rho_{eq}^n(\mathbf{r},\Omega) \tag{12}$$

for n = 1,2, involving the equilibrium solvent density of each state. According to Figure 1, the solvent reorganization energy is then defined by

$$\lambda = \langle \Delta E\rangle_1 - \Delta F = \langle \Delta V\rangle_1 - \Delta F_S \tag{13}$$

It turns out therefore that, in our MDFT formalism, the computation of the thermodynamics quantities of interest requires only two minimizations instead of the complete thermodynamics path linking states 1 and 2 that is necessary in molecular simulations.

Note that if the Marcus Gaussian approximation is invoked (or, stated differently, the linear response approximation), the following relations apply

$$\Delta F_S = \frac{1}{2}(\langle \Delta V\rangle_1 + \langle \Delta V\rangle_2) \tag{14}$$

$$\lambda = \frac{1}{2}(\langle \Delta V\rangle_1 - \langle \Delta V\rangle_2) \tag{15}$$

which makes it possible to bypass the costly direct computation of ΔF_S. They will be the subject of discussion later on.

3. APPLICATION TO SOLVATION IN ACETONITRILE

We have applied our MDFT formalism to molecular solvation in acetonitrile, a solvent that has been considered as a paradigm for polar nonprotic solvent on experimental as well as theoretical grounds. We have used the three-site molecular model of Edwards et al.[86] involving a unified description of the methyl group. Because the model is linear, only the angles θ and ϕ need to be considered, and the molecules' orientation can be described by a unit orientation vector $\mathbf{\Omega}$.

3.1. Obtaining the Direct Correlation Function. We first performed a several nanoseconds MD simulation of liquid acetonitrile at T = 300 K and a density of n_0 = 0.01154 particles/Å^3. The system was composed of 3000 molecules in a cubic box of 63.8 Å. The corresponding pair distribution function, $h^{(int)}(r, \cos\theta_1, \cos\theta_2, \phi_2 - \phi_1)$, computed in the so-called intermolecular frame where z is taken along the intermolecular vector, is displayed in Figure 2 for different relative orientations of the two molecules. The corresponding direct correlation function in **k**-space, $c(k, \cos\theta_1, \cos\theta_2, \phi_2 - \phi_1)$, obtained by solving eq 10 using a Gauss−Legendre discretization of order 6 for cos θ and a regular grid of order 12 for ϕ, is shown in Figure 2; see ref 47 for details. Due to the finite sample size, these functions are ill-defined at very small k-values; they were extrapolated quadratically below k = 0.5 Å^{-1}, with the additional condition of matching exact thermodynamics relationships at k = 0 (see the Appendix). To clarify this point and illustrate the overall quality of the computed c's, we display in Figure 3 the three first spherical invariant projections $\hat{c}_{000}(k)$, $\hat{c}_{110}(k)$, and $\hat{c}_{112}(k)$, pertinent to dipolar symmetry; See refs 24−26, 37, 44, and 45 and the Appendix for their

dx.doi.org/10.1021/jp210817s | J. Phys. Chem. B 2012, 116, 2504−2512

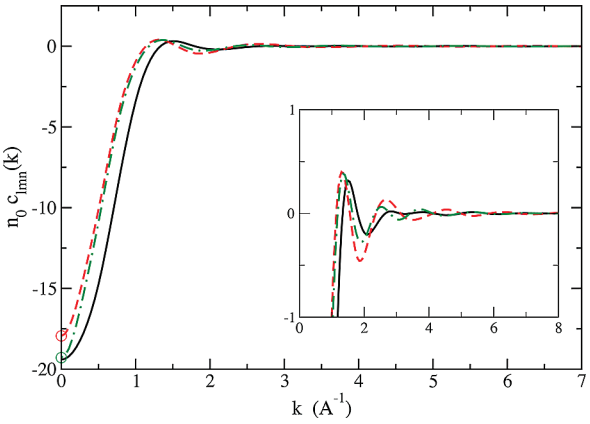

Figure 3. Spherical invariant components of the direct correlation function of acetonitrile in **k**-space (multiplied by the bulk density n_0); $\hat{c}_{000}(k)$ (black solid line), $\hat{c}_{110}(k)$ (red dashed line), and $\overline{c}_{112}(k)$ (green dashed–dotted line). The colored circles indicate the expected $k = 0$ values, eqs 17 and 18. The inlet shows an enlargement at a scale similar to that in Figure 2.

definition. The expected "exact" values at $k = 0$ are also displayed

$$n_0\hat{c}^{ex}_{000}(0) = 1 - \frac{1}{n_0 k_B T \chi_T} \tag{16}$$

$$n_0\hat{c}^{ex}_{110}(0) = 3\left(1 - \frac{\epsilon + 2}{\epsilon - 1}y\right) \tag{17}$$

$$n_0\hat{c}^{ex}_{112}(0) = -3y \tag{18}$$

with $y = \beta n_0\mu^2/9\epsilon_0$, $\mu = 4.6$ D as the dipole moment of acetonitrile in the Edwards et al. model, and $\epsilon = 33$ as the corresponding dielectric constant.[86] χ_T refer to the isothermal compressibility of the model. Because that quantity was never computed directly, to our knowledge, and because we have never computed it, we decided to stick to our extrapolation of $\hat{c}_{000}(k)$ at small k, which proves safer than that for the other angular-dependent components.[87] The corresponding functions in **r**-space are shown in Figure 4. Their determination

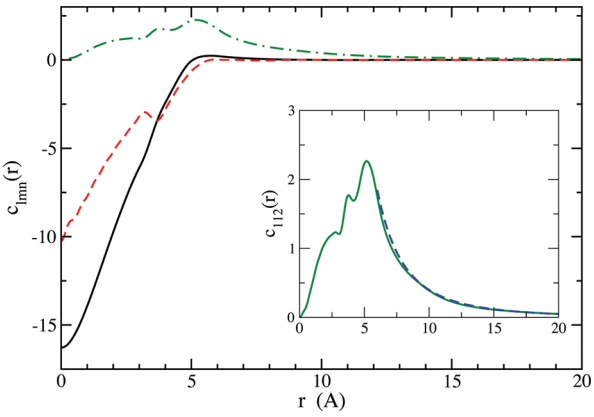

Figure 4. Spherical invariant components of the direct correlation function of acetonitrile in **r**-space; $c_{000}(r)$ (black solid line), $c_{110}(r)$ (red dashed line), and $c_{112}(r)$ (green dashed–dotted line). The inlet compares the dipolar component to the expected asymptotic behavior, $c_{112}(r) \simeq -k_B T\mu^2/4\pi\epsilon_0 r^3$ (dashed blue line).

involves a zero-order inverse Hankel transform for $c_{000}(r)$ and $c_{110}(r)$ and a second-order one for $c_{112}(r)$.[37] As expected, the two former functions are short-ranged and vanish beyond $r >$ 5–6 Å, whereas $c_{112}(r)$ is long-ranged and behaves as the long-range dipole–dipole potential $c_{112}(r) = -\beta\mu^2/4\pi\epsilon_0 r^3$ beyond the same distance. This property insures the correct dielectric behavior. Overall, the combination of the direct numerical results of the MOZ inversion for $k > 0.5$ Å^{-1} and smooth extrapolation to exact values at $k = 0$ appears as a reasonable procedure to get the angular c-functions over the whole k-range.

3.2. Solvation of Molecular Solutes. With the c-function being known and stored in the intermolecular frame, it can be easily transformed to the laboratory frame to give $c(\mathbf{k},\Omega_1,\Omega_2)$ for any **k**-vector and any couples of orientation, and it can used in the excess part of the functional, eq 8. The functionals in eqs 3–6 can then be minimized in the presence of the external potential field created by a microscopic solute, placed at the center of a parallelipedic box. The gradients are defined by eqs 7 and 8. The minimization is performed in fact with respect to a "fictitious wave function", $\psi(\mathbf{r},\mathbf{\Omega}) = \rho(\mathbf{r},\mathbf{\Omega})^{1/2}$, in order to prevent the density from becoming negative. For all of the solutes described below, we used a cubic box with typically $L =$ 30 Å, and the density functional was minimized using a 64^3 points Cartesian grid for positions and a Gauss–Legendre grid of 32 angles for orientations (a Gauss–Legendre quadrature for $\cos\theta$ between −1 and 1 and a regularly spaced grid between 0 and 2π for ϕ). The calculations thus involve ∼8 million variables to be minimized simultaneously and 64 3D-FFTs to be performed per minimization step (using the very efficient fftw3 package[88]). For minimization, we used the L-BFGS quasi-Newton optimization routine,[89] which requires as input free energy and gradients. The calculation were performed on a single processor of a standard desktop workstation or laptop. The convergence turned out to be fast, requiring at most 25–30 iterations, so that despite the important number of FFTs to be handled, one complete minimization only takes a few minutes on a single laptop processor. This is probably due to the fact that the highly multidimensional function to be minimized is perfectly convex and close to harmonicity near the minimum. Note that a standard free-energy perturbation calculation using a similar box containing 500 acetonitrile molecules and, typically, 10 integration windows and 10000 simulation steps per windows would require ∼20 h using the same single processor.

This procedure is illustrated in Figures 5 and 6 for the solvation of the *N*-methylacetamide molecule (NMA: CH_3–NH–CO–CH_3), the paradigm for a peptide bond. We used the Jorgensen's Lennard-Jones and charge parameters with a unified description of the two methyl groups.[90] In Figure 5, we compare the different solute-site/solvent-center of mass (COM) pair distribution functions obtained after functional minimization to the same quantities computed by MD simulations (using one NMA molecule immersed in 500 acetonitrile molecules). The agreement is found to be excellent. Furthermore, in order to illustrate the capability of MDFT to provide, at the end of the minimization, 3D densities in addition to pair distribution functions, we show in Figure 6 a two-dimensional map of the local polarization density, plotted in the molecular plane. We have represented, in fact, the modulus of the polarization, $P(\mathbf{r}) = |\mathbf{P}(\mathbf{r})|$, with

$$\mathbf{P}(\mathbf{r}) = \int d\mathbf{\Omega}\, \mathbf{\Omega}\rho_{eq}(\mathbf{r}, \mathbf{\Omega}) \tag{19}$$

dx.doi.org/10.1021/jp210817s | J. Phys. Chem. B 2012, 116, 2504–2512

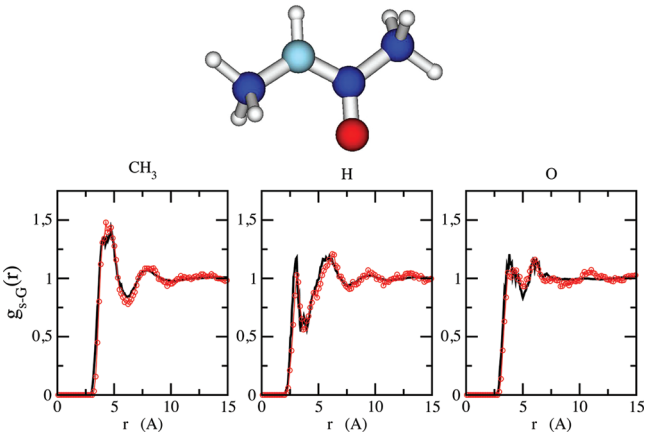

Figure 5. Solute-site/solvent-COM pair distribution function for different atomic sites of *N*-methylacetamide computed by MDFT (solid black lines) or MD simulations (dotted red lines). A molecular picture of NMA is given on top of the figure, and the sites are labeled on each panel.

and we have done so for the two possible isomers of the NMA molecule, that is, the trans and cis forms. In the two cases, the highest polarization region is observed around the N−H bond and is thus displaced from cis to trans. The organization around the C═O bond remains rather similar in the two forms. Obtaining the same two- or three-dimensional information from MD simulations requires extremely long runs to accumulate sufficient statistics in each elementary cubic bin.

The capability of MDFT to predict solvation free energies in addition to the microscopic solvent structure is illustrated for monovalent ions in refs 47 and 48.

3.3. Charge-Transfer Reactions. We borrow our applications of MDFT to charge-transfer reactions from the work of Kumar and Maroncelli[91] and Ladanyi and Maroncelli.[92] These authors have studied the solvation thermodynamics and the solvation dynamics of various photosensitive dye molecules in acetonitrile using MD simulations. They have considered, in particular, coumarin 153, which undergoes an S_0 to S_1 electronic transition upon photoexcitation and for which high-quality experimental data exist. This molecule is depicted in Figure 7 (its geometry and charge distribution in the S_0 or S_1 state may be found in the Supporting Information of ref 91; see ref 41 of this paper). They have also designed various "toy models" that make it possible to vary systematically the degree of charge transfer for a given molecular geometry and thus to modulate the coupling to the solvent. Among them, we will consider their "benzene model" in which, starting from a neutral, apolar benzene molecule, charge switches of one or minus one electron are operated on the ring carbon atoms to create either an octupolar, quadrupolar, dipolar, or charged excited species. See Figure 8; The corresponding excited states are denoted by O, Q, D, and C, respectively. In concordance with the theoretical arguments of Sec. 2.2, each solute was placed at the center of a cubic box, and the functional 3−6 was minimized with either the ground or excited state partial charges distribution.

Figure 9 displays the correlation obtained for the whole solute series between the solvent reorganization energies computed by MDFT, using the exact formula in eq 13 and the MD simulation values provided by Landanyi and Maroncelli from the energy gap fluctuations.[92] The agreement appears indeed very good and certainly within the MD

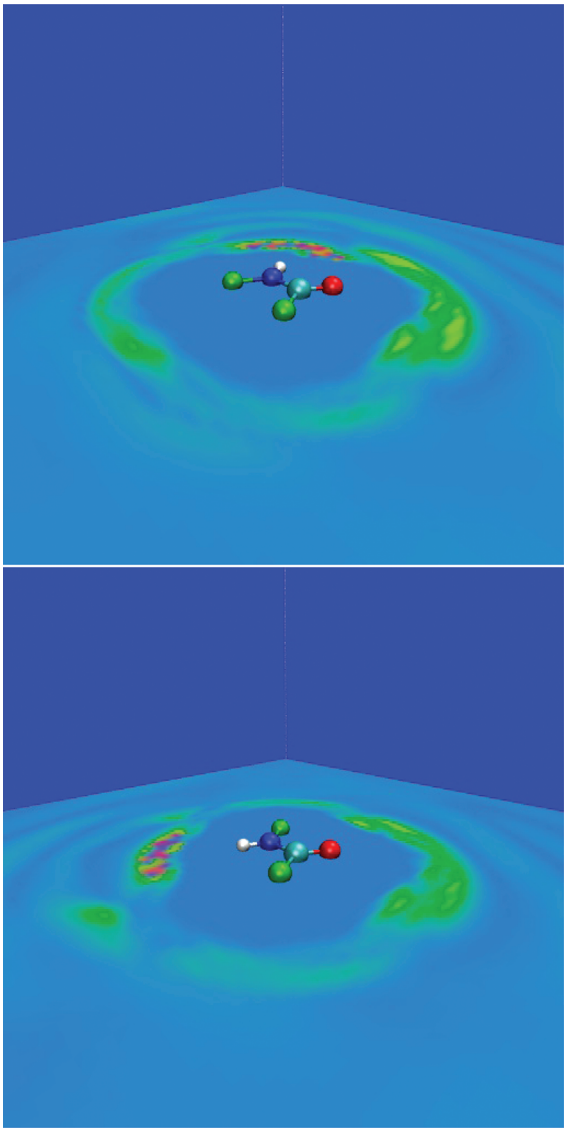

Figure 6. Representation of the solvent polarization density in the plane of the *N*-methylacetamide molecule for the cis and trans isomers (top and bottom figures, respectively; blue = 0 and red = highest values).

statistical errors that are inherent to that quantity (although not stipulated).

At last, Figure 10 provides a verification of the linear response relationships of eqs 14 and 15. All quantities being computed consistently by MDFT for the whole molecule series, the linear response approximation for the solvation free-energy difference, eq 15, is correlated with the exact value, $\Delta F_S = F_{eq}^2 - F_{eq}^1$. The correlation appears almost perfect, which proves that solvation in acetonitrile, at least for the type of solute considered, is completely in the linear response (or Gaussian) regime. Such a situation might not always be the case, even for simple polar aprotic solvents.[4] For aqueous solutions, there is also mounting evidence that many charge-transfer reactions might not be well-described by simple Gaussian statistics; see, for example, ref 93.

4. CONCLUSION

In continuation to refs 47 and 48, we have presented in this paper a molecular density functional theory (MDFT) approach

dx.doi.org/10.1021/jp210817s | J. Phys. Chem. B 2012, 116, 2504−2512

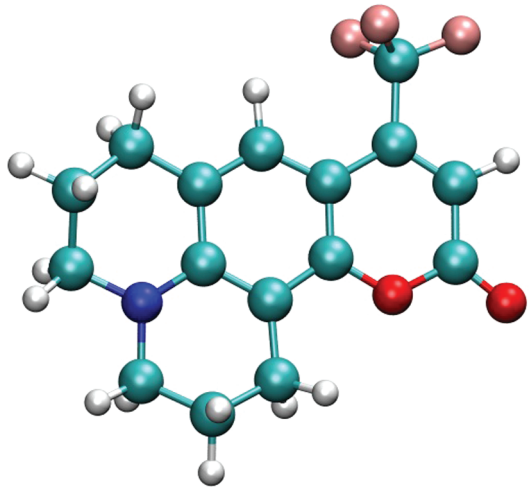

Figure 7. Molecular representation of coumarin 153. A complementary representation of the charge distribution in the S_0 state, and of the charge variation between S_0 and S_1, may be found in ref 91.

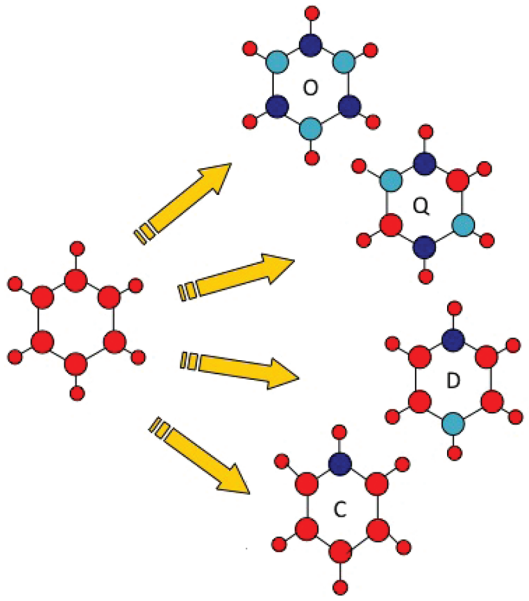

Figure 8. Schematic representation of the "benzene model" of Maroncelli and colleagues.[91,92] The dark blue and light blue disks indicate a change of atomic charge of +e or −e, respectively.

to solvation in molecular solvents, which includes two steps, (1) extracting the unknown excess free energy from the computation of the angular-dependent pair distribution using a long molecular dynamics simulation of the pure solvent and subsequent inversion of the MOZ equation to get the direct correlation function and (2) minimizing the corresponding functional on a three-dimensional grid in the presence of an arbitrary solute. We have shown that the two steps are technically feasible using angular grids to handle the orientational dependence and FFTs to go back and forth between direct and Fourier space. Futhermore, it provides at the same time three-dimensional solvent density maps, quantities that also require very long statistical averages in MD. To complement our previous works, we have shown that the approach is applicable to the computation of electron-transfer properties such as reaction free energies and solvent reorganization free energies. Very good agreement was found

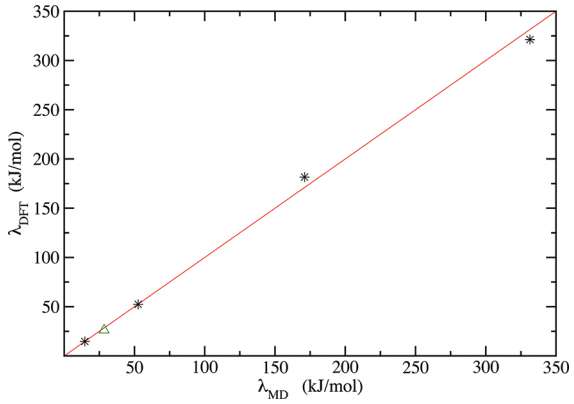

Figure 9. Correlation of the reorganization energy computed by MDFT to those determined by MD by Ladanyi and Maroncelli.[92] The stars correspond, in increasing order, to the photoexcitation to a O, Q, D, or C molecule (Figure 8). The triangle corresponds to coumarin 153.

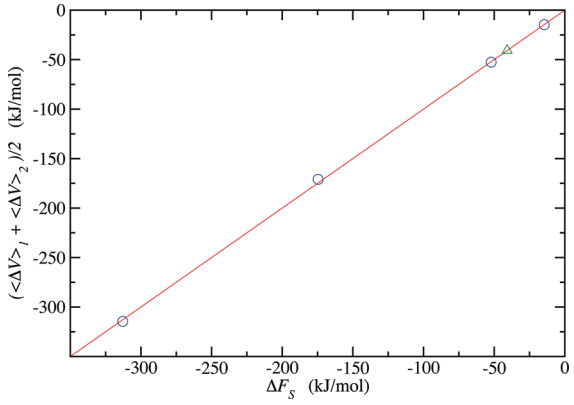

Figure 10. Correlation between the linear response approximation for the solvent contribution to the reaction free energy, eq 15, and the "exact" definition, eq 11 (all quantities computed by MDFT). The circles correspond, in increasing order, to the photoexcitation to a C, D, Q, and O molecule (Figure 8). The triangle corresponds to coumarin 153.

with respect to available MD results for a sample of photoexcitable molecules in acetonitrile. This represents, to our knowledge, the first application of classical DFT to the modeling of charge-transfer processes in solution.

The next steps of MDFT will be to consider other aprotic and protic solvents, such as acetone and water. For the latter, it is already certain that the homogeneous reference fluid approximation discussed in the paper, limited to two-body solvent correlations, cannot be completely satisfactory and that the inclusion of other terms in the functional, such as nonlocal three-body density terms, cannot be avoided.[48] It will be important also to generalize the approach to solvent mixtures and ionic solutions and to include the electronic polarizability of both the solvent and the solute. Extensions of MDFT in all of those directions are currently in progress.

APPENDIX: CORRECTING THE DIRECT CORRELATION FUNCTION AT SMALL *K*

As mentioned in the text, due to finite size effects, the angular-dependent *h*- or *c*-functions are ill-defined close to $k = 0$. For acetonitrile, we find that the problem arises below $k_{min} = 0.5$ Å^{-1}. Above that value, the *c*-functions obtained by inversion of

dx.doi.org/10.1021/jp210817s | J. Phys. Chem. B 2012, 116, 2504−2512

the MOZ relation are smooth and apparently well-converged. What we have done in a first step is to extrapolate quadratically each $c(k,\xi_1,\xi_2,\phi_{12})$ (with $\xi_i = \cos\theta_i$) below k_{min} to get a first reasonable guess between 0 and k_{min}.

Next, we have computed the first spherical invariant projections defined in the intermolecular frame by

$$\hat{c}_{lmn}(k) = \frac{a_{lmn}}{8\pi}\int_{-1}^{1} d\xi_1\, d\xi_2 \int_0^{2\pi} d\phi\, \Phi_{lmn}(\xi_1, \xi_2, \phi)\, c(k, \xi_1, \xi_2, \phi) \quad (20)$$

with $a_{000} = 1$, $a_{110} = 3$, $a_{112} = 3/2$ and

$$\Phi_{000}(\xi_1, \xi_2, \phi) = 1 \quad (21)$$

$$\Phi_{110}(\xi_1, \xi_2, \phi) = \xi_1\xi_2 + (1-\xi_1)^{1/2}(1-\xi_2)^{1/2}\cos\phi \quad (22)$$

$$\Phi_{112}(\xi_1, \xi_2, \phi) = 2\xi_1\xi_2 - (1-\xi_1)^{1/2}(1-\xi_2)^{1/2}\cos\phi \quad (23)$$

The exact values of $\hat{c}^{ex}_{000}(0)$, $\hat{c}^{ex}_{110}(0)$, and $\hat{c}^{ex}_{112}(0)$ can be inferred from thermodynamic properties, namely, the isothermal compressibility and the dielectric constant, using relations derived in ref 37

$$n_0 k_B T \chi_T = 1 + n_0\hat{h}_{000}(0) = \frac{1}{1 - n_0\hat{c}_{000}(0)} \quad (24)$$

in refs 45, 94, and 95

$$\frac{\epsilon - 1}{\epsilon + 2} = y\left(1 + \frac{n_0}{3}\hat{h}_{110}(0)\right) = y\left(1 - \frac{n_0}{3}\hat{c}_{110}(0)\right)^{-1} \quad (25)$$

and in ref 80 (using $\epsilon_\perp(k=0) = \epsilon$)

$$\frac{\epsilon - 1}{3} = y\left(1 - \frac{n_0}{3}\hat{h}_{-}(0)\right) = y\left(1 + \frac{n_0}{3}\hat{c}_{-}(0)\right)^{-1} \quad (26)$$

In these equations, $y = \beta n_0\mu^2/9\epsilon_0$, $\hat{h}_{-} = \hat{h}_{112} - \hat{h}_{110}$, $\hat{c}_{-}$ has a similar definition. One can easily get from this the relations in eqs 16−18. The experimental isothermal compressibility of acetonitrile at 298.15 K is 1.15×10^{-9} Pa^{-1}. That of the three-site acetonitrile model that we used is not known. Using the experimental value instead, with $n_0 = 0.011543$, yields $n_0\hat{c}_{000}(0) = -17.3$. Furthermore $\epsilon = 33$, and $\mu = 4.16$ D,[86] such that $y = 6.43$, $n_0\hat{c}_{110}(0) = -17.94$, and $n_0\hat{c}_{112}(0) = -19.29$.

Accounting for the above exact relations, we can correct the angular-dependent c-functions previously defined and extrapolated at small k's in order to fulfill them exactly at $k = 0$. To this end, we define a corrected function

$$c_{cor}(k, \xi_1, \xi_2, \phi_{12}) = c(k, \xi_1, \xi_2, \phi_{12}) + \exp(-R_c^2k^2/2) \sum_{lmn} (\hat{c}^{ex}_{lmn}(0) - \hat{c}_{lmn}(0))\Phi_{lmn}(\xi_1, \xi_2, \phi_{12}) \quad (27)$$

with lmn = 000, 110, and 112 and R_c an arbitrary value adjusted to produce a smooth curve leaving $c(k,\xi_1,\xi_2,\phi_{12})$ unchanged above $k_{min} = 0.5$ Å^{-1}; We converged to $R_c = 3$ Å. We did not correct here for the (undetermined) isothermal compressibility (000 component). It appears however that the mere quadratic extrapolation of $\hat{c}_{000}(k)$ at small k is quite reasonable and much more precise than that for the other angular-dependent components.[87]

The resulting spherical invariant projections are displayed in Figures 3 and 4 in both **k**- and **r**-space.

AUTHOR INFORMATION

Corresponding Author

*E-mail: daniel.borgis@ens.fr.

Notes

The authors declare no competing financial interest.

ACKNOWLEDGMENTS

D.B. acknowledges financial support from the Agence Nationale de la Recherche within the SIMISOL project, ANR- 09-SYSC-012.

REFERENCES

(1) Kollman, P. *Chem. Rev.* **1993**, *93*, 2395.
(2) Torrie, G. M.; Valleau, J. *J. Comput. Phys.* **1977**, *23*, 187.
(3) Valleau, J. In *Classical and Quantum Dynamics in Condensed Phase Simulations*; Berne, B. J., Ciccotti, G., Cocker, D., Eds.; World Scientific Co.: River Edge, NJ, 1998; p 97.
(4) Carter, E. A.; Hynes, J. T. *J. Phys. Chem.* **1989**, *93*, 2184−2187.
(5) Ciccotti, G. In *Classical and Quantum Dynamics in Condensed Phase Simulations*; Berne, B. J., Ciccotti, G., Cocker, D., Eds.; World Scientific Co.: River Edge, NJ, 1998; page 159.
(6) Shivakumar, D.; Deng, Y. Q.; Roux, B. *J. Chem. Theory Comput.* **2009**, *5*, 919.
(7) Roux, B.; Simonson, T. *Biophys. Chem.* **1999**, *78*, 1.
(8) Simonson, T. *Rep. Prog. Phys.* **2003**, *66*, 737.
(9) Honig, B.; Nichols, A. *Science* **1995**, *268*, 1144.
(10) Baker, N. A.; Sept, D.; Joseph, S.; Holst, M. J.; McCammon, J. A. *Proc. Natl. Acad. Sci. U.S.A.* **2001**, *98*, 10037.
(11) Marchi, M.; Borgis, D.; Lévy, N.; Ballone, P. *J. Chem. Phys.* **2001**, *114*, 4377.
(12) Allen, R.; Hansen, J. P.; Melchionna, S. *Phys. Chem. Chem. Phys.* **2001**, *3*, 4177.
(13) Allen, R.; Hansen, J. P. *J. Phys.: Condens. Matter* **2003**, *14*, 11981.
(14) Cheng, L. T.; Dzubiella, J.; McCammon, J. A. *J. Chem. Phys.* **2007**, *127*, 084503.
(15) Cheng, L. T. T.; Xie, Y.; Dzubiella, J.; McCammon, J. A.; Che, J.; Li, B. *J. Chem. Theory Comput.* **2009**, *5*, 257.
(16) Chandler, D.; Hendersen, H. *J. Chem. Phys.* **1972**, *57*, 1930.
(17) Hirata, F.; Rossky, P. J. *Chem. Phys. Lett.* **1981**, *83*, 329.
(18) Hirata, F.; Pettitt, B. M.; Rossky, P. J. *J. Chem. Phys.* **1982**, *77*, 509.
(19) Reddy, G.; Lawrence, C. P.; Skinner, J. L.; Yethiraj, A. *J. Chem. Phys.* **2003**, *119*, 13012.
(20) Beglov, D.; Roux, B. *J. Phys. Chem. B* **1997**, *101*, 7821.
(21) Kovalenko, A.; Hirata, F. *Chem. Phys. Lett.* **1998**, *290*, 237.
(22) F. Hirata, E. *Molecular Theory of Solvation*; Kluwer Academic Publishers, Dordrecht, The Netherlands, 2003.
(23) Yoshida, N.; Imai, T.; Phongphanphanee, S.; Kovalenko, A.; Hirata., F. *J. Phys. Chem. B* **2009**, *113*, 873.
(24) Blum, L.; Torruella, A. J. *J. Chem. Phys.* **1972**, *56*, 303.
(25) Blum, L. *J. Chem. Phys.* **1972**, *57*, 1862.
(26) Patey, G. N. *Mol. Phys.* **1977**, *34*, 427.
(27) Carnie, S. L.; Patey, G. N. *Mol. Phys.* **1982**, *47*, 1129.
(28) Fries, P. H.; Patey, G. N. *J. Chem. Phys.* **1985**, *82*, 429.
(29) Richardi, J.; Fries, P. H.; Krienke, H. *J. Chem. Phys.* **1998**, *108*, 4079.
(30) Richardi, J.; Millot, C.; Krienke, H. *J. Chem. Phys.* **1999**, *110*, 1138.
(31) Dyer, K. M.; Perkyns, J. S.; Pettitt, B. M. *J. Chem. Phys.* **2007**, *127*, 194506.

(32) Dyer, K. M.; Perkyns, J. S.; Stell, G.; Pettitt, B. M. *J. Chem. Phys.* **2008**, *129*, 104512.
(33) Chandler, D. *Phys. Rev. E* **1993**, *48*, 2898.
(34) Ten Wolde, P. R.; Sun, S. X.; Chandler, D. *Phys. Rev. E* **2001**, *65*, 011201.
(35) Varilly, P.; Patel, A. J.; Chandler, D. *J. Chem. Phys.* **2010**, *134*, 074109.
(36) Maggs, A. C.; Everaers, R. *Phys. Rev. Lett.* **2006**, *96*, 230603.
(37) Hansen, J. P.; McDonald, I. R. *Theory of Simple Liquids*; Academic Press: London, 1989.
(38) Evans, R. *Adv. Phys.* **1979**, *28*, 143.
(39) Evans, R. In *Fundamental of Inhomogeneous Fluids*; Henderson, D., Ed.; Marcel Dekker: New York, 1992.
(40) Wu, J. *AIChE J.* **2006**, *52*, 1169.
(41) Wu, J.; Li, Z. *Annu. Rev. Phys. Chem.* **2007**, *58*, 85.
(42) Biben, T.; Hansen, J. P.; Rosenfeld, Y. *Phys. Rev. E* **1998**, *57*, R3727.
(43) Oleksy, A.; Hansen, J. P. *J. Chem. Phys.* **2010**, *132*, 204702.
(44) Ramirez, R.; Gebauer, R.; Mareschal, M.; Borgis, D. *Phys. Rev. E* **2002**, *66*, 306.
(45) Ramirez, R.; Borgis, D. *J. Phys. Chem. B* **2005**, *109*, 6754.
(46) Ramirez, R.; Mareschal, M.; Borgis, D. *Chem. Phys.* **2005**, *319*, 261.
(47) Gendre, L.; Ramirez, R.; Borgis, D. *Chem. Phys. Lett.* **2009**, *474*, 366.
(48) Zhao, S.; Ramirez, R.; Vuilleumier, R.; Borgis, D. *J. Chem. Phys.* **2011**, *134*, 194102.
(49) Zhao, S.; Jin, Z.; Wu, J. *J. Phys. Chem. B* **2011**, *115*, 6971.
(50) Coalson, R. D.; Walsh, A. M.; Duncan, A.; Ben-Tal, N. *J. Chem. Phys.* **1995**, *102*, 4584.
(51) Coalson, R. D.; Duncan, A. *J. Phys. Chem. B* **1996**, *100*, 2612.
(52) Coalson, R. D.; Beck, T. L. In *Encyclopedia of Computational Chemistry*; von Rague Schleyer, P. J. Wiley & Sons: New York, 1998.
(53) Azuara, C.; Lindahl, E.; Koehl, P. *Nucleic Acids Res.* **2006**, *34*, 38.
(54) Azuara, C.; Orland, H.; Bon, M.; Koehl, P.; Delarue, M. *Biophys. J.* **2008**, *95*, 5587.
(55) Marcus, R. A. *J. Chem. Phys.* **1956**, *24*, 966.
(56) Marcus, R. A. *J. Chem. Phys.* **1956**, *24*, 979.
(57) Levich, V. G.; Dogonadze, R. R. *Dokl. Acad. Nauk. SSSR* **1959**, *124*, 123.
(58) Newton, M. D. *Annu. Rev. Phys. Chem.* **1986**, *35*, 437−480.
(59) Kuznetsov, A. M. *Charge Transfer in Physics, Chemistry, and Biology*; Gordon and Breach: Reading, U.K., 1995.
(60) Kuznetsov, A. M.; Ulstrup, J. *Electron transfer in chemistry and Biology: An Introduction to the Theory*; Wiley and Sons: Chichester, U.K., 1999.
(61) Warshel, A. *J. Phys. Chem.* **1982**, *86*, 2218−2224.
(62) Hwang, J. K.; Warshel, A. *J. Am. Chem. Soc.* **1987**, *109*, 715−720.
(63) Kuharsky, R. A.; Bader, J. S.; Chandler, D. *J. Chem. Phys.* **1988**, *89*, 3248−3257.
(64) Carter, E. A.; Hynes, J. T. *J. Phys. Chem.* **1989**, *93*, 2184−2187.
(65) Borgis, D.; Hynes, J. T. *J. Chem. Phys.* **1991**, *94*, 3619.
(66) Marchi, M.; Gehlen, J.; Chandler, D.; Newton, M. *J. Am. Chem. Soc.* **1993**, *115*, 4178.
(67) Azzouz, H.; Borgis, D. *J. Chem. Phys.* **1993**, *98*, 7361.
(68) Simonson, T. *Proc. Natl. Acad. Sci. U.S.A.* **2002**, *99*, 6544.
(69) Ceccarelli, M.; Marchi, M. *J. Phys. Chem. B* **2003**, *107*, 5630−5641.
(70) Sterpone, F.; Ceccarelli, M.; Marchi, M. *J. Phys. Chem. B* **2003**, *107*, 11208−11215.
(71) Kornyshev, A. A.; Sutmann, G. *Electrochim. Acta* **1996**, *42*, 1564.
(72) Kornyshev, A. A.; Sutmann, G. *Electrochim. Acta* **1997**, *42*, 2801.
(73) Bagchi, B.; Chandra, A. *Adv. Chem. Phys.* **1991**, *80*, 1.
(74) Fried, L. E.; Mukamel, S. *J. Chem. Phys.* **1990**, *93*, 932.
(75) Fonseca, T.; Ladanyi, B. *J. Chem. Phys.* **1990**, *93*, 8148.
(76) M. S. Skaf, T. F.; Ladanyi, B. *J. Chem. Phys.* **1993**, *98*, 8929.
(77) Bopp, P. A.; Kornyshev, A. A.; Sutmann, G. *Phys. Rev. Lett.* **1996**, *76*, 1281.
(78) Bopp, P. A.; Kornyshev, A. A.; Sutmann, G. *J. Chem. Phys.* **1998**, *109*, 1939.
(79) Raineri, F. O.; Friedman, H. L. *Adv. Chem. Phys.* **1999**, *107*, 81.
(80) Raineri, F. O.; Friedman, H. L. *J. Chem. Phys.* **1993**, *98*, 8910.
(81) Raineri, F. O.; Resat, H.; Perng, B. C.; Hirata, F.; Friedman, H. L. *J. Chem. Phys.* **1994**, *100*, 1477.
(82) Chandra, A.; Wei, D.; Patey, G. N. *J. Chem. Phys.* **1993**, 2068.
(83) Chandra, A.; Wei, D.; Patey, G. N. *J. Chem. Phys.* **1993**, *4926*, 99.
(84) Matyushov, D. *J. Chem. Phys.* **2004**, *120*, 7532.
(85) Hansen, J. P. In *The Physics and Chemistry of Aqueous Ionic Solutions*; Bellissent-Funel, M. C., Neilson, G. W., Eds.; Kluwer Academic Publishers: Dortrecht, The Netherlands, 1987.
(86) Edwards, D. M.; Madden, P. A.; McDonald, I. R. *Mol. Phys.* **1984**, *51*, 1141.
(87) Gendre, L. *Density functional theory of molecular liquids: Application to solvation in polar solvents*. PhD thesis, Université d'Evry-Val-d'Essonne, Evry, France, 2008.
(88) Frigo, M.; Johnson, S. G. *Proc. IEEE* **2005**, *93*, 216.
(89) Byrd, R. H.; Lu, P.; Nocedal, J. *SIAM J. Sci. Comput.* **1995**, *16*, 1190.
(90) Jorgensen, W.; Gao. *J. Am. Chem. Soc.* **1988**, *110*, 4212.
(91) Kumar, P. V.; Maroncelli, M. *J. Chem. Phys.* **1995**, *103*, 3038.
(92) Ladanyi, B. M.; Maroncelli, M. *J. Chem. Phys.* **1998**, *109*, 3204.
(93) Blumberger, J. *J. Am. Chem. Soc.* **2008**, *130*, 16065−16068.
(94) Ramshaw, J. D. *J. Chem. Phys.* **1972**, *57*, 2684.
(95) Ramshaw, J. D. *J. Chem. Phys.* **1977**, *66*, 3134.